MiR-1188 at the imprinted *Dlk1-Dio3* domain acts as a tumor suppressor in hepatoma cells

Wei Cui[a], Zhijun Huang[a], Hongjuan He[a], Ning Gu[a], Geng Qin[a], Jie Lv[a], Tao Zheng[a], Kenkichi Sugimoto[b], and Qiong Wu[a]

[a]School of Life Science and Technology, State Key Laboratory of Urban Water Resource and Environment, Harbin Institute of Technology, Harbin, Heilongjiang 150001, China; [b]Department of Cell Science, Faculty of Graduate School of Science and Technology, Niigata University, Nishi-ku, Niigata 950-2181, Japan

ABSTRACT **The aberrant expression of microRNAs (miRNAs) has frequently been reported in cancer studies; miRNAs play roles in development, progression, metastasis, and prognosis. Recent studies indicate that the miRNAs within the *Dlk1-Dio3* genomic region are involved in the development of liver cancer, but the role of miR-1188 in hepatocellular carcinoma (HCC) and the pathway by which it exerts its function remain largely unknown. Here we demonstrate that miR-1188 is significantly down-regulated in mouse hepatoma cells compared with normal liver tissues. Enhanced miR-1188 suppresses cell proliferation, migration, and invasion in vitro and inhibits the tumor growth of HCC cells in vivo. Moreover, overexpressed miR-1188 promotes apoptosis, enhances caspase-3 activity, and also up-regulates the expression of Bax and p53. MiR-1188 directly targets and negatively regulates *Bcl-2* and *Sp1*. Silencing of *Bcl-2* and *Sp1* exactly copies the proapoptotic and anti-invasive effects of miR-1188, respectively. The expression of apoptosis- and invasion-related genes, such as *Vegfa*, *Fgfr1*, and *Rprd1b*, decreases after enhancement of miR-1188, as determined by gene expression profiling analysis. Taken together, our results highlight an important role for miR-1188 as a tumor suppressor in hepatoma cells and imply its potential role in cancer therapy.**

Monitoring Editor
Jonathan Chernoff
Fox Chase Cancer Center

Received: Dec 4, 2014
Revised: Feb 9, 2015
Accepted: Feb 13, 2015

INTRODUCTION

MicroRNAs (miRNAs) are conserved short RNAs that suppress protein expression through base pairing with the 3′-untranslated region (UTR) of target mRNAs (Jewer *et al.*, 2012). Increasing evidence suggests that miRNAs play important roles in multiple pathological processes and have significant functions as both tumor suppressors and oncogenes (Ren *et al.*, 2014; Shen *et al.*, 2014; Su *et al.*, 2014). As a new class of genomic information, miRNA dysregulation can provide insight into new carcinogenic pathways and opportunities for biomarker and therapeutic target discovery (Denoyelle *et al.*, 2014; Roderburg and Luedde, 2014).

Hepatocellular carcinoma (HCC) is one of the most common cancers and contributes markedly to increased cancer-related death (Cha and Dematteo, 2005; Aravalli *et al.*, 2008). Altered miRNA expression is observed in HCCs collected from cohorts in different studies. Furthermore, several dysregulated miRNAs have been shown to regulate cell growth, apoptosis, migration, or invasion (Xiong *et al.*, 2010; Lu *et al.*, 2011; Xie *et al.*, 2013; Liu *et al.*, 2014; Wang *et al.*, 2014). These findings suggest that dysregulation of miRNA may be associated with hepatocarcinogenesis. More extensive investigations are required to elucidate the role of miRNAs in the development of HCC in order to identify which ones might be used as novel prognosis predictors or as therapeutic targets for HCC (Zhang *et al.*, 2012; Yang *et al.*, 2013b).

Sp1 is a member of the Sp/Kruppel-like factor (KLF) family (Yasuda *et al.*, 2002). A previous study reported that *Sp1* was critically involved in cell growth and tumorigenesis (Lou *et al.*, 2005). Aberrant expression of *Sp1* is regulated by miRNAs; this has been observed in various cancers, including hepatocellular carcinomas, breast cancer, and gastric cancer (Xu *et al.*, 2011a, 2012; Banerjee *et al.*, 2012). *Bcl-2*, as an oncogene, has been implicated in

This article was published online ahead of print in MBoC in Press (http://www.molbiolcell.org/cgi/doi/10.1091/mbc.E14-11-1576) on February 18, 2015.

Address correspondence to: Qiong Wu (kigo@hit.edu.cn).

Abbreviations used: HCC, hepatocellular carcinoma; miRNA, microRNA; PFA, paraformaldehyde; qRT-PCR, quantitative real-time PCR; UTR, untranslated region.

apoptosis and tumorigenesis (Janumyan *et al.*, 2003; Kelly and Strasser, 2011). It has been shown that miR-15 and miR-16 can down-regulate *Bcl-2* in many types of cancer, including gastric cancer and chronic lymphocytic leukemia (Cimmino *et al.*, 2005; Xia *et al.*, 2008). Moreover, the introduction of miR-29 dramatically repressed the ability of HCC cells to form tumors and promoted HCC cells apoptosis by targeting *Bcl-2* (Xiong *et al.*, 2010).

The *Mus musculus* intron-encoded miR-1188 is located in the *Dlk1-Dio3* imprinted miRNA cluster (Glazov *et al.*, 2008). Previous research showed that overexpression of this miRNA cluster is positively correlated with HCC stem cell markers and associated with a conventional biomarker for liver cancer (Luk *et al.*, 2011). In the present study, low miR-1188 expression was found in a hepatoma cell line when compared with normal liver tissue. Cell proliferation, Transwell cell migration and invasion assays, and in vitro colony formation assays demonstrated that overexpression of miR-1188 suppressed hepatoma cell proliferation and invasion. Moreover, overexpressed miR-1188 promoted apoptosis and enhanced caspase-3 activity; it also up-regulated Bax and p53 protein expression. In addition, miR-1188 suppressed the ability of HCC cells to form tumors in vivo. Furthermore, we used a luciferase reporter assay and Western blot to confirm that miR-1188 might function as a tumor suppressor in hepatoma by targeting *Sp1* and *Bcl-2*. Gene expression profiling analysis of enhanced miR-1188 cells revealed changes in apoptosis- and invasion-related genes such as *Vegfa*, *Fgfr1*, and *Rprd1b*. Our findings will help to elucidate the functions of miR-1188 and its roles in HCC.

RESULTS

The expression of miR-1188 was down-regulated and inversely correlated with *Bcl-2*/*Sp1* in Hepa1-6 cells

MiR-1188 is located in the *Meg8* transcripts from a maternally expressed gene in the *Dlk1-Dio3* imprinted cluster on mouse chromosome 12qF1. According to miRBase data and sequence alignment, there is only one base difference between human and mouse miR-1188 (Figure 1A).

Expression of miR-1188 was determined in hepatoma cells and the major organs of mice. Quantitative real-time PCR (qRT-PCR) showed that miR-1188 was widely expressed in the major organs (Figure 1B), and markedly down-regulated in Hepa1-6 cells, when compared with normal liver tissue (Figure 1D). We analyzed miR-1188 in the liver by in situ hybridization; mature miR-1188 localized in the cytoplasm (Figure 1C). We hypothesized that enhanced *Bcl-2* and *Sp1* expression in hepatoma cells could be a result of reduced miR-1188 expression, so we examined *Bcl-2* and *Sp1* mRNA and protein levels in Hepa1-6 and normal liver tissue. Figure 1E shows that, compared with normal liver tissue, the expression of *Bcl-2* and *Sp1* was significantly higher in Hepa1-6 cells.

MiR-1188 suppressed cell proliferation, migration, and invasion in vitro

To investigate whether miR-1188 plays a role in the development and progression of liver cancer, we transfected cells with miR-1188 mimics, stable negative controls (SNCs), inhibitor, or negative control (NC). Figure 2A shows that miR-1188 expression in cells transfected with mimics was up-regulated hundredsfold, whereas in cells transfected with inhibitor, the expression decreased by almost 95%. Use of 3-(4,5-dimethylthiazol-2-yl)-2,5-diphenyltetrazolium bromide (MTT) assays demonstrated that cell viability was reduced by 25% in cells transfected with mimics compared with SNC at 96 h (Figure 2B), suggesting a proliferation-suppressive function of miR-1188. Moreover, colony formation assays showed that enhanced miR-1188 levels suppressed colony formation, whereas miR-1188 inhibitor increased colony formation compared with the NC group (Figure 2C). These data indicate that miR-1188 could inhibit the growth of hepatoma cells.

Changes in cell morphology are important parameters for cancer invasion and migration. We measured and analyzed the morphology (area) of cells transfected with mimics or SNC in each well of a 24-well plate. The cell size distribution showed significant differences between mimics and SNC-treated cells (Figure 2D). MiR-1188, remarkably, inhibited the cell area by twofold overall compared with SNC, showing that miR-1188 triggers morphological changes in hepatoma cells.

To evaluate whether miR-1188 is biologically involved in the modulation of tumor cell migration and invasion in Hepa1-6 cells, we performed wound-healing and Transwell matrix penetration assays. Figure 2E shows that Hepa1-6 cells transfected with the miR-1188 mimics displayed lower migratory speed than cells transfected with SNC. Consistent with this result, Transwell migration assays showed that the number of cells that migrated after transfection with miR-1188 inhibitor was ~1.6-fold higher than for NC. Furthermore, the invasion capability of Hepa1-6 cells increased 3.5-fold as a result of miR-1188 inhibition. Opposite results were clearly observed in the mimics group (Figure 2, F and G), indicating an inhibitory effect of miR-1188 on migration and invasion of hepatoma cells. These results suggest that miR-1188 represses traits key to the development of metastasis in hepatoma cells in vitro.

Up-regulation of miR-1188 induced apoptosis and activated caspase-3

Figure 3B shows that transient transfection of miR-1188 mimics resulted in significantly increased caspase-3 activation, which is a key indication of cells undergoing apoptosis. We next observed that up-regulation of miR-1188 enhanced apoptosis by nearly 70-fold compared with SNC in Hepa1-6 cells (Figure 3A). Taken together, these data indicate that up-regulation of miR-1188 induced hepatoma cell apoptosis. To explore the molecules involved in apoptosis, we measured the protein expressions of Bax, Bcl-2, and p53 in enhanced miR-1188 cells. Figure 3C shows that overexpression of miR-1188 significantly suppressed the expression of Bcl-2 in Hepa1-6 cells. However, the expression of Bax and p53 was up-regulated. Taken together, these results indicate that miR-1188 might induce apoptosis partially by targeting *Bcl-2*.

However, the expression of other genes regulated by miR-1188 might also play important roles in tumorigenesis. Gene expression profiling analysis of miR-1188–overexpressing Hepa1-6 cells revealed changes in levels of apoptosis- and tumorigenesis-related genes. Functional grouping analysis using the Database for Annotation, Visualization, and Integrated Discovery (DAVID) showed that 15 of the genes differentially regulated by enhanced miR-1188 were related to apoptosis and migration. The expression of these genes was changed in enhanced miR-1188 cells, indicating that they are in potential relationship with miR-1188 (Figure 3D). Many related genes, such as *Vegfa*, *Fgfr1*, and *Rprd1b*, were down-regulated after enhanced miR-1188 expression. Genes up-regulated by enhanced miR-1188 included tumor suppressors CD44, *Dapk1*, and *Apaf1* (Haraguchi *et al.*, 2000; Lee *et al.*, 2005; Williams *et al.*, 2013).

MR-1188 directly targets Bcl-2 and Sp1

To begin to understand the molecular mechanisms underlying the proapoptotic and anti–migratory/invasive effects of miR-1188, we postulated that *Bcl-2* and *Sp1* might represent targets of miR-1188,

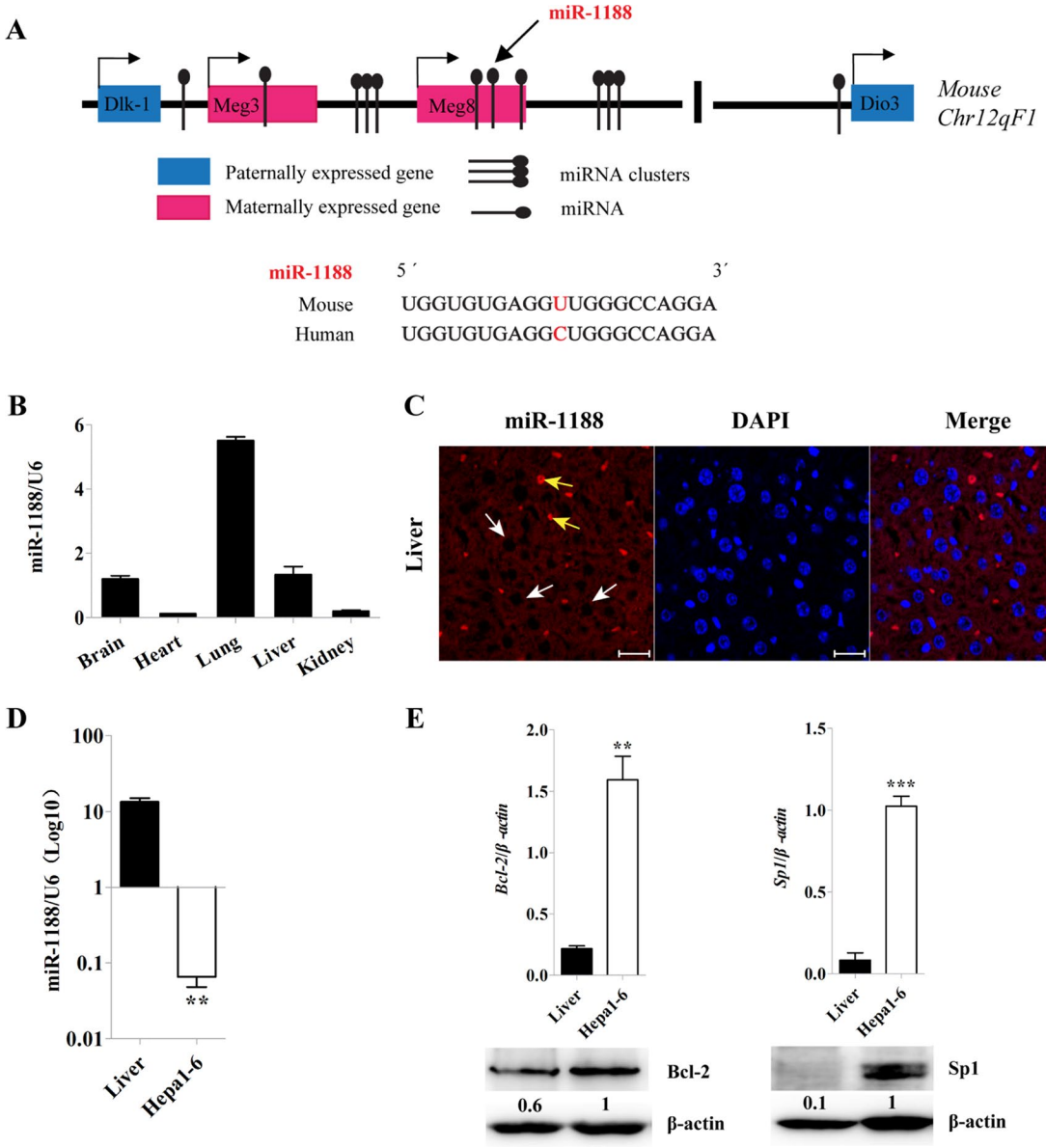

FIGURE 1: The location and expression of miR-1188 in mouse. (A) *M. musculus* miR-1188 is located on the maternally expressed gene in a *Dlk1-Dio3* imprinted cluster. (B, D) qRT-PCR analysis showed the relative levels of miR-1188 in 6-wk-old mice and Hepa1-6 cells. Relative miRNA levels were determined after normalization with U6. (C) Expression of miR-1188 in liver tissue using in situ hybridization (viewed by confocal microscopy). White arrows indicate mature miR-1188 localization in the cytoplasm, and yellow arrows represent blood cells. DAPI staining (blue) was used to visualize the nuclei; scale bars, 10 μm. (E) qRT-PCR and immunoblot analyses showed the relative levels of *Bcl-2* and *Sp1* in Hepa1-6 cells and liver tissue. Each value was determined in triplicate; $^{**}p < 0.01$, $^{***}p < 0.001$.

containing in their 3′-UTRs potential binding sites for the miRNA (Figure 4, A and B).

To address whether these two genes were directly regulated by miR-1188, we performed luciferase reporter assays. The wild-type *Bcl-2* and *Sp1* 3′-UTRs, as well as mutant forms, were cloned into a pMIR-REPORT luciferase vector. Hepa1-6 cells were transiently transfected with *Bcl-2* or *Sp1* 3′-UTRs and miR-1188 mimics or SNC. *Renilla* luciferase vector was used for normalization. The results showed that miR-1188 inhibited the luciferase activity of the wild-type *Bcl-2* and *Sp1* 3′-UTRs but not the mutant *Bcl-2* and *Sp1* 3′-UTRs, suggesting that miR-1188 could directly target *Bcl-2* and *Sp1* (Figure 4, C and D).

To assess further whether miR-1188 repressed *Bcl-2* or *Sp1* expression in the mouse hepatoma intracellular environment, we analyzed *Bcl-2* and *Sp1* expression in Hepa1-6 cells after transfection with miR-1188 mimics or inhibitor. MiR-1188 changed the expression of *Bcl-2* and *Sp1* at the posttranscriptional level (Figure 4, E and F). Western blot assays showed that Bcl-2 and Sp1 protein levels were dramatically decreased in the miR-1188 mimics–treated group. Conversely, levels of Bcl-2 and Sp1 were increased in miR-1188 inhibitor groups compared with NC treatment (Figure 4G). To further confirm that Sp1 was negatively regulated by miR-1188, we analyzed Sp1 expression by immunofluorescence. Sp1 was predominantly located in the nucleus 48 h after the transfection of miR-1188

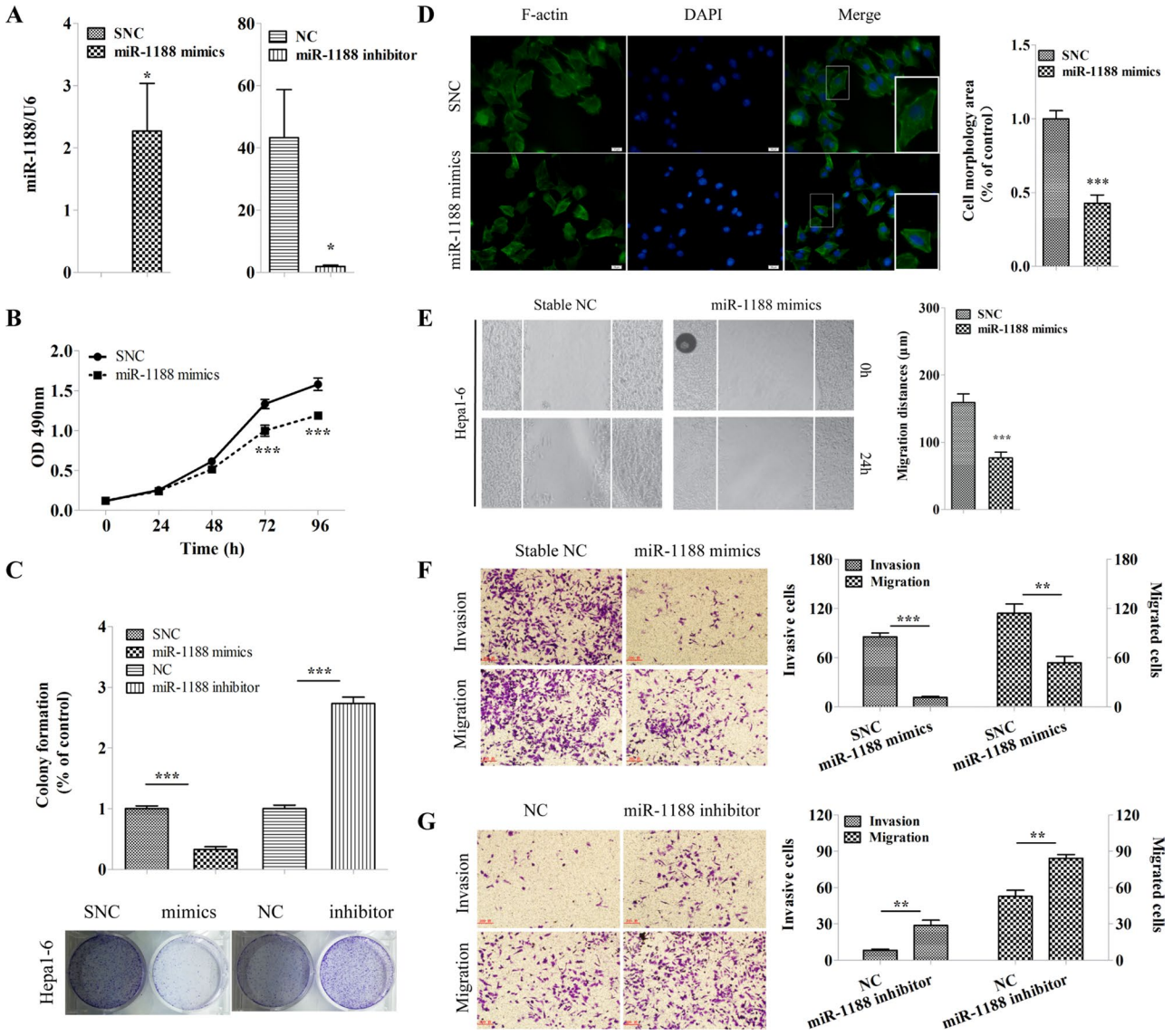

FIGURE 2: MiR-1188 suppressed cell proliferation, migration, and invasion in Hepa1-6 cells in vitro. (A) qRT-PCR analysis showed the relative levels of miR-1188 after Hepa1-6 cells were transfected with mimics or inhibitor. Relative miRNA levels were determined after normalization with U6. (B) Representative growth curves corresponding to Hepa1-6 cells transfected with SNC or miR-1188 mimics. (C) Colonies grown from Hepa1-6 cells transfected with mimics, SNC, inhibitor, or NC were counted. Percentage of control means the ratio of the experimental group to the control group, with each control defined at a value of 1 for statistical analysis. (D) Immunofluorescence staining of Alexa Fluor 488–conjugated phalloidin, which is a high-affinity probe for F-actin (green), in Hepa1-6 cells transfected with SNC or mimics for 24 h (viewed by fluorescence microscope). Enlarged images of the boxed area are shown in the bottom right corner of the merge image; scale bars, 20 μm. Cell areas (morphology) were calculated and analyzed by image analysis. Ten randomly selected regions were analyzed. (E) Confluent monolayers of cells transfected with SNC or mimics were wounded and incubated for an additional 24 h. The migration distances were calculated. (F, G) Migration and invasion of Hepa1-6 cells transfected with SNC, mimics, NC, or inhibitor. Error bars represent the SE obtained from three independent experiments; *$p < 0.05$, **$p < 0.01$, ***$p < 0.001$.

mimics, and the level of Sp1 was significantly reduced compared with SNC (Figure 4H). Collectively these results suggest that *Bcl-2* and *Sp1* are direct targets of miR-1188, and miR-1188 affects Bcl-2 and Sp1 expression by directly binding to their 3′-UTR target regions.

MiR-1188 mediated apoptosis and invasion by modulating Bcl-2 and Sp1 levels

To investigate further the relationship between miR-1188 and its targets, we knocked down *Bcl-2* and *Sp1* by RNA interference. Expression of Bcl-2 and Sp1 was down-regulated, as shown by qRT-PCR and Western blot (Figure 5, A–D). To confirm further that Sp1 was regulated by small interfering RNA (siRNA), we analyzed Sp1 expression using immunofluorescence (unpublished data). Subsequently, we used *Sp1*–5′-UTR 588 and *Bclx2*-5′-UTR 1926 siRNAs for further experiments. As expected, knockdown of *Sp1* markedly inhibited cell proliferation as determined by MTT assays; the suppression rate was 25 and 34% at 72 and 96 h, respectively (Figure 5E). Similarly, *Sp1* knockdown reduced cell migration and invasion in Hepa1-6 cells (Figure 5F). These results suggested that knockdown

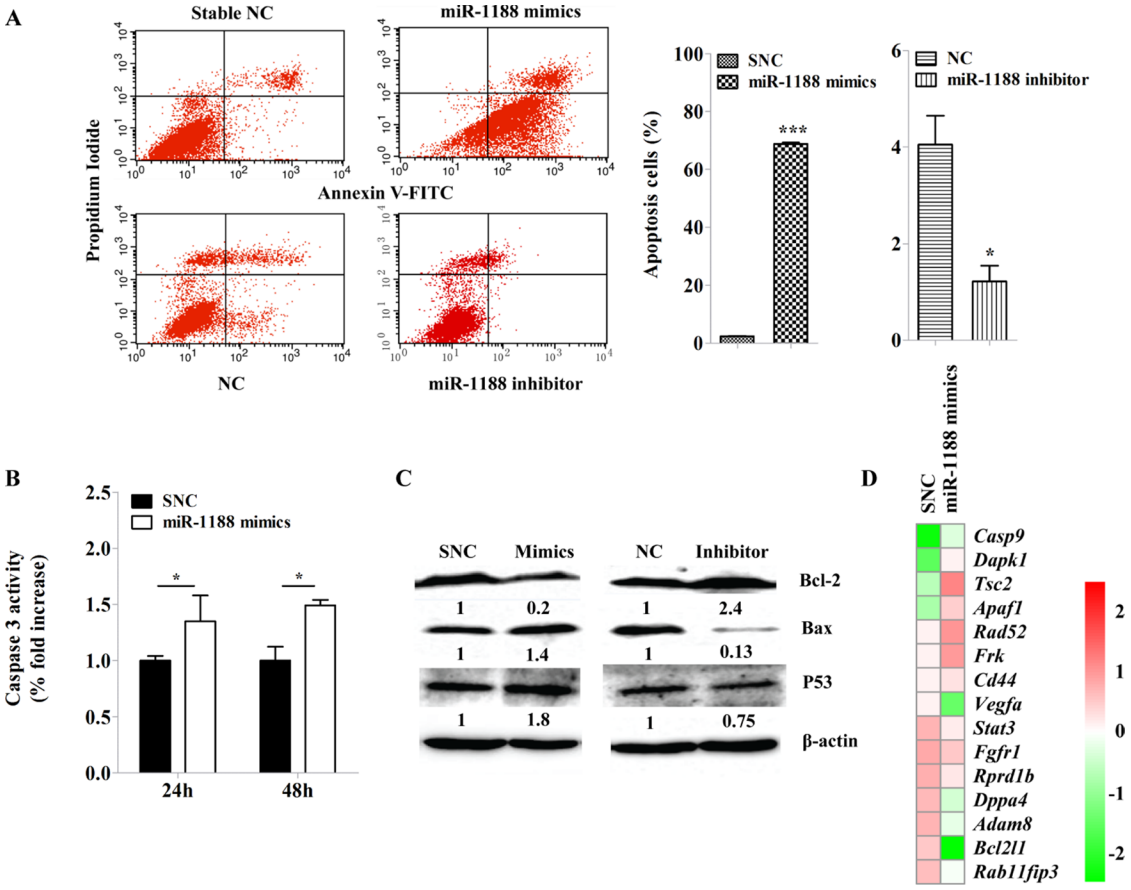

FIGURE 3: MiR-1188 induces apoptosis in Hepa1-6 cells in vitro. (A) Annexin V–FITC/PI staining of cells treated with scramble or miR-1188 mimics or inhibitor for 20 h. (B) MiR-1188 increased the activation of caspase-3. (C) Immunoblot analysis of Bcl-2, Bax, and P53 in Hepa1-6 cells transfected with miR-1188 mimics or inhibitor. (D) Heat map of gene expression profile data for 15 genes from Hepa1-6 cells transfected with SNC or miR-1188 mimics. The values were centered and scaled columnwise using the pheatmap R package and sorted by the ratio of mimics and SNC. Color from red to green represents genes that were down-regulated. Error bars represent the SE obtained from three independent experiments; *$p < 0.05$, ***$p < 0.001$.

of *Sp1* changed the biological behavior of Hepa1-6 cells in much the same pattern as miR-1188 up-regulation. In addition, Figure 5G shows that suppression of *Bcl-2* by siRNA promoted apoptosis and miR-1188 inhibitor led to reduced apoptosis, whereas miR-1188 inhibitor rescued apoptosis caused by suppression of *Bcl-2* in cells cotransfected with inhibitor and siRNA compared with cells cotransfected with siRNA alone.

Western blots showed that the levels of Bcl-2 and Sp1 were reduced in hepatoma cells transfected with either miR-1188 mimics or *Bcl-2*/*Sp1* siRNAs (Figures 5, H and I). In contrast, down-regulation of miR-1188 elevated the expression of both Bcl-2 and Sp1. More significantly, miR-1188 inhibitor rescued the protein expression of Bcl-2 or Sp1 in cells cotransfected with inhibitor and siRNA compared with cells cotransfected with siRNA alone (Figure 5, H and I). These results indicate that Bcl-2 or Sp1 might be involved in mediating the tumor-suppressive function of miR-1188.

MiR-1188 inhibits tumor growth in vivo

The data showing that miR-1188 negatively modulated hepatoma cell proliferation in vitro prompted us to ask whether the miRNA acted as an antitumor factor in vivo. To address this issue, we measured dynamic growth of subcutaneously xenografted hepatoma tumors in BALB/c-nu mice over 18 d. Our results showed that mice bearing control and miR-1188–overexpressing Hepa1-6 cells on the left and right flanks, respectively, began to exhibit differences in tumor growth between the two sides in the first week, and the difference increased until the experimental endpoint (Figure 6, A and B). This trend was confirmed by the weights of the dissected tumors (Figure 6C), strongly suggesting a marked deceleration of tumor cell proliferation by miR-1188.

qRT-PCR revealed that the expression of miR-1188 was increased in hepatoma xenograft tumor tissues treated with miR-1188 mimics compared with those treated with SNC (Figure 6D). Western blot showed that expression of Bcl-2 and Sp1 was decreased in tumor tissues containing mimics compared with SNC (Figure 6E). Correlation analysis indicated that there was a significant inverse correlation between miR-1188 and Bcl-2/Sp1 protein expression, with $R = –0.834$ and $–0.667$, respectively (Figure 6F). Furthermore, tumor tissues were embedded in paraffin and then stained for histological examination. To observe the localization of Sp1 protein in tumor tissues, we performed fluorescence immunohistochemical staining. Green fluorescence indicated Sp1 protein expression (Figure 6G), which was located in the nucleus. Together these data support our in vitro findings that miR-1188 was inversely correlated with *Bcl-2*/*Sp1* and that *Bcl-2* and *Sp1* were potential target genes for miR-1188.

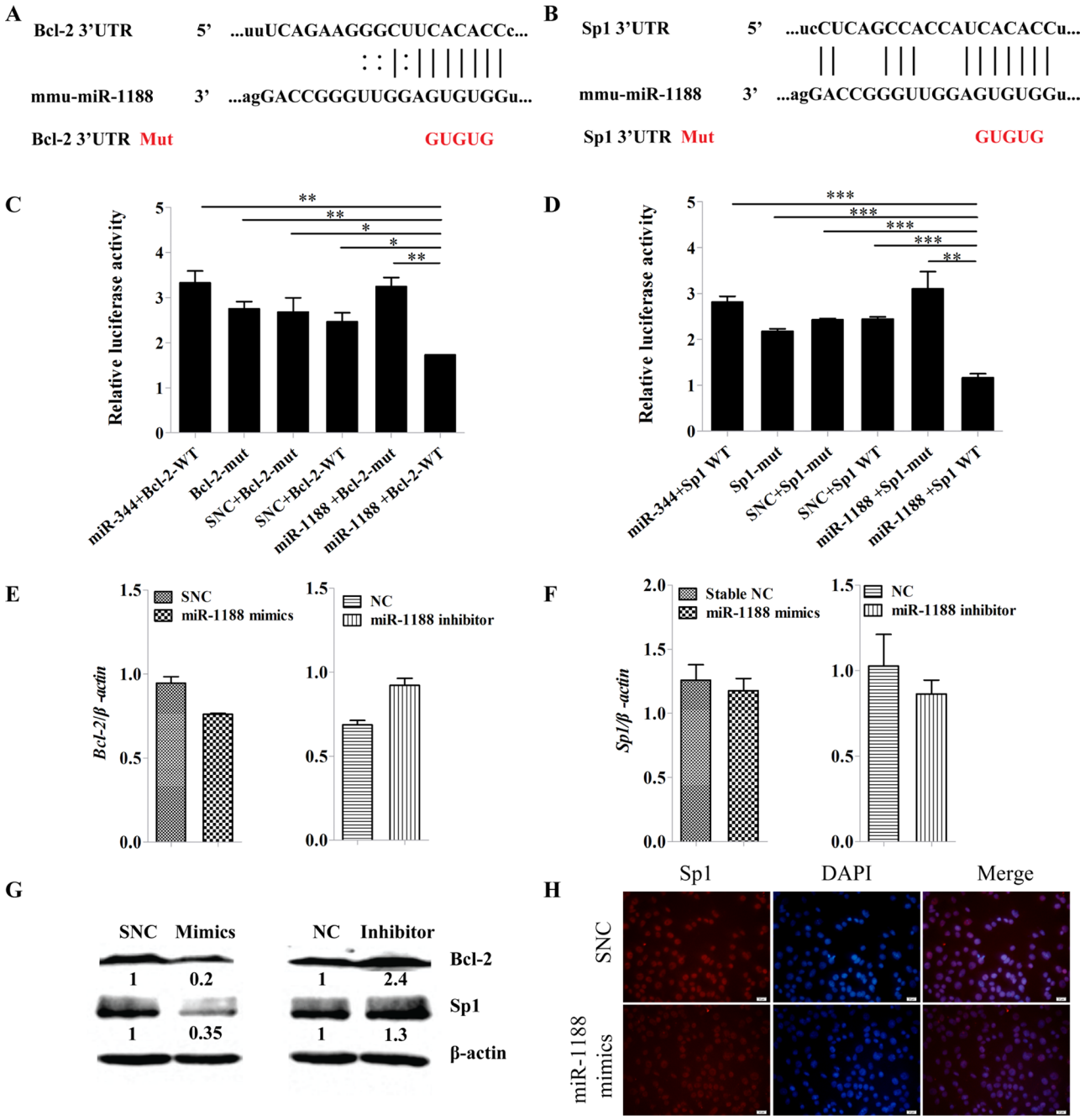

FIGURE 4: Bcl-2 and Sp1 are direct targets of miR-1188. (A, B) Computer prediction of the binding of miR-1188 to the 3′-UTRs of mouse *Bcl-2* and *Sp1*. The mutated base sequences in the luciferase reporter assays are shown in red. (C, D) Relative luciferase activity of the indicated *Bcl-2* or *Sp1* reporter constructs. MiR-344 was used as a positive control and does not target *Bcl-2*/*Sp1*. (E, F) qRT-PCR analysis shows the relative levels of *Bcl-2* and *Sp1* after transfection of miR-1188 mimics or miR-1188 inhibitor into Hepa1-6 cells. (G) Immunoblot analysis of Bcl-2 and Sp1 proteins in Hepa1-6 cells transfected with miR-1188 mimics or inhibitor. (H) Immunofluorescence staining showed that Sp1 expression was regulated by miR-1188. Overexpression of miR-1188 suppressed Sp1 expression in Hepa1-6 cells. DAPI staining (blue) was used to visualize nuclei; scale bars, 20 μm. Error bars represent the SE obtained from three independent experiments; *$p < 0.05$, **$p < 0.01$, ***$p < 0.001$.

DISCUSSION

MiR-1188 is located in transcripts of *Meg8*, which has been identified as a maternally expressed gene in the mouse *Dlk1-Dio3* imprinted cluster. The imprinted miRNA cluster is involved in the pathogenesis of different diseases (Benetatos *et al.*, 2013) and modulates important pathways such as mitogen-activated protein kinase (MAPK), Wnt, JAK-STAT, P53, and many more (Iliopoulos *et al.*, 2009; Swarbrick *et al.*, 2010; Gattolliat *et al.*, 2011). For example, miR-127 inhibited cell proliferation and migration by targeting MAPK4 in gastric cancer cells (Guo *et al.*, 2013). Down-regulated miR-136 targets AEG-1 and Bcl-2 in human glioma, which promotes the apoptosis of glioma (Yang *et al.*, 2012). Other evidence suggests that miRNAs at the imprinted *Dlk1-Dio3* cluster are also involved in the development of liver cancer. MiR-433 is a potent inhibitor of

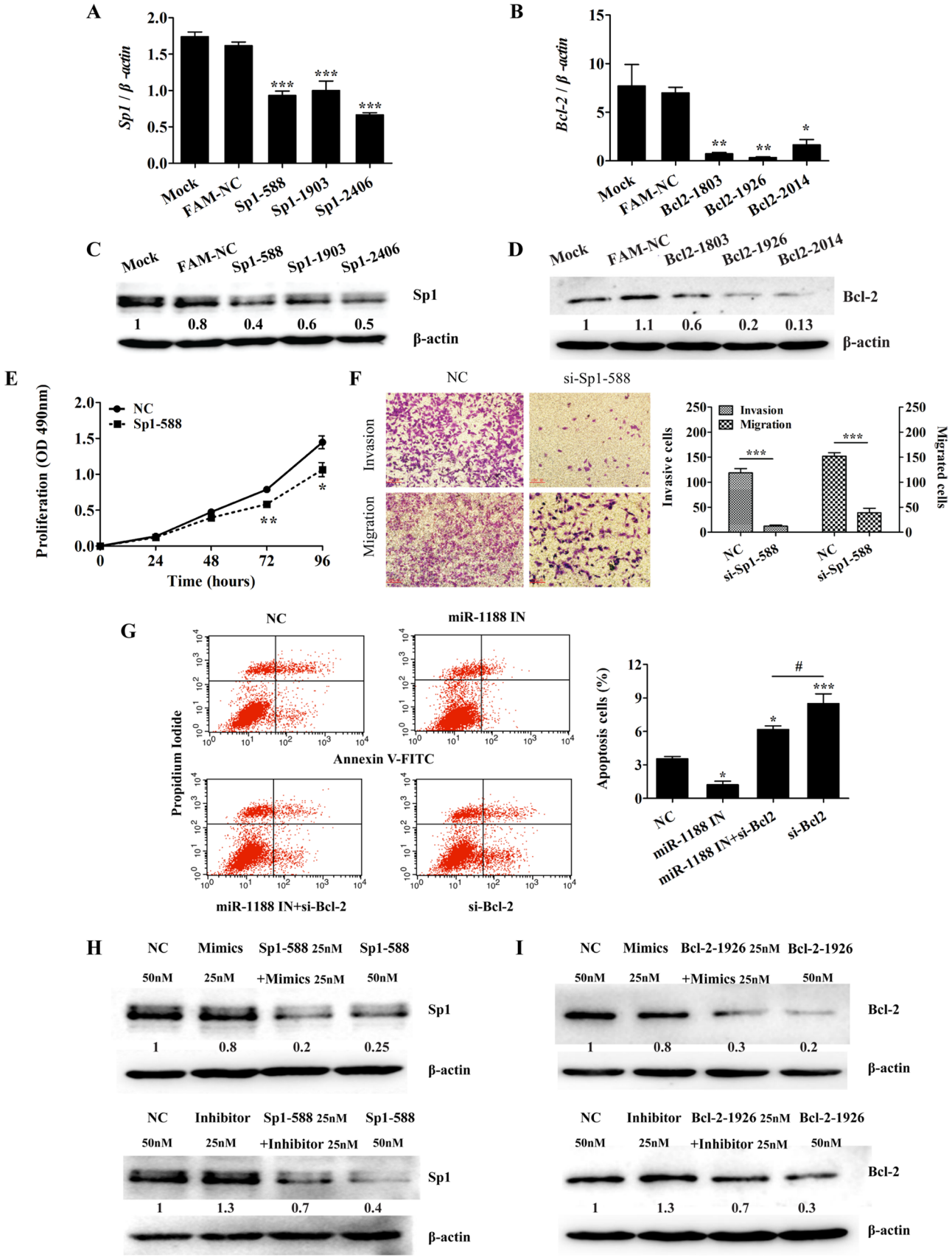

FIGURE 5: MiR-1188 mediates invasion and apoptosis by modulating Bcl-2 and Sp1 levels. (A, B) qRT-PCR analysis showed the relative levels of *Bcl-2* and *Sp1* in Hepa1-6 cells transfected with NC or siRNA, respectively. (C, D) Immunoblot analysis of Bcl-2 and Sp1 in Hepa1-6 cells transfected with siRNA. (E) Representative growth curves corresponding to Hepa1-6 cells transfected with NC or si-Sp1-588. (F) Migration and invasion of Hepa1-6 cells

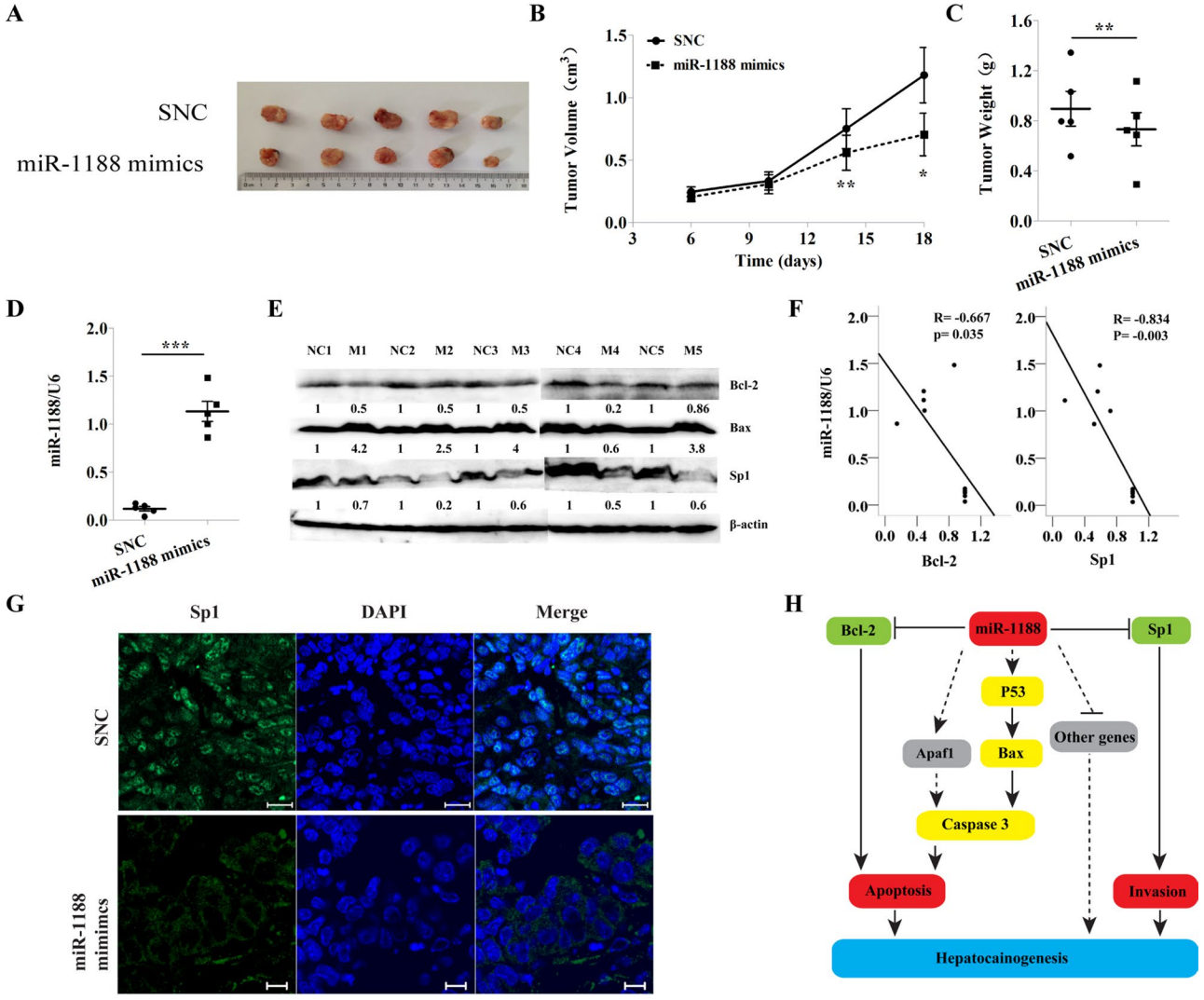

FIGURE 6: MiR-1188 inhibited hepatoma tumor growth in vivo. (A) Hepa1-6 cells were injected subcutaneously into the left and right flanks of nude mice and the transplanted tumors harvested ($n = 5$). (B, C) The weight and volume of the harvested transplanted tumors. (D) The expression of miR-1188 in the tumors as found by qRT-PCR. (E) The expression of Bax, Bcl-2, and Sp1 in the tumors as revealed by immunoblot. (F) Inverse correlation between miR-1188 and Sp1 or Bcl-2 protein level in the tumors. Statistical analysis was performed using Pearson's *R*, and *R* and *P* values are as shown. (G) Immunohistochemistry showed the Sp1 expression (viewed by confocal microscopy). DAPI staining (blue) was used to visualize nuclei; Scale bars, 20 μm. (H) Schematic diagram showing the signaling network in which miR-1188 is involved. Error bars represent the SE obtained from three independent experiments; $*p < 0.05$, $**p < 0.01$, $***p < 0.001$.

HCC cell migration through its action on CREB1 (Yang *et al.*, 2013a). MiR-127 can result in the formation of hepatocellular carcinoma by decreasing apoptosis rates (Tryndyak *et al.*, 2009). MiR-370, which is also located among the *Meg8* transcripts, can inhibit the growth and metastasis of HCC cells in vivo (Xu *et al.*, 2013). In our study, miR-1188 could regulate cell proliferation, apoptosis, migration, and invasion and suppress tumor growth by directly targeting *Bcl-2* and *Sp1* in hepatoma cells, suggesting that miR-1188 may also participate in the development of liver cancer.

The present study reports, for the first time, the functional effect of miR-1188 as a novel tumor suppressor in hepatoma cells. MiR-1188 was expressed at a low level in hepatoma cells compared with normal liver tissue, which suggested that down-regulation of the expression level of miR-1188 was correlated with cancer progression. Overexpression of miR-1188 in hepatoma cell lines reduced cell viability and invasion ability, promoted apoptosis, and suppressed tumorigenicity, suggesting a tumor suppressor activity. Therefore, miR-1188 might serve an important function in apoptosis

transfected with NC or si-Sp1-588. (G) Annexin V–FITC/PI staining of cells cotransfected with NC or miR-1188 inhibitor and/or si-Bcl-2 for 20 h. (H, I) Immunoblot analysis showed that the levels of Bcl-2 and Sp1 were changed in Hepa1-6 cells transfected with miR-1188 mimics, miR-1188 inhibitor, si-Bcl-2, or si-Sp1. More significantly, miR-1188 inhibitor rescued the level of Bcl-2 or Sp1 in cells cotransfected with inhibitor and siRNAs compared with cells transfected with siRNA alone. Error bars represent the SE obtained from three independent experiments; $*p < 0.05$, $**p < 0.01$, $***p < 0.001$.

and invasion pathways. Furthermore, we characterized *Bcl-2* and *Sp1* as functional targets of miR-1188 and proved their involvement (Figure 6H), thereby indicating a fundamental role of miR-1188 in tumorigenesis and suggesting the potential application of miR-1188 in prognosis prediction and cancer therapy.

Most cases of HCC arise in cirrhotic livers with persistent inflammation. Further understanding of the mechanistic link between inflammation and HCC would help to identify potential therapeutic targets for HCC. *Sp1* is a key transcriptional regulator that exerts a variety of biological functions. Elevated expression of *Sp1* has been observed in HCC (Lietard *et al.*, 1997; Yang *et al.*, 2001; Fang *et al.*, 2007). Of interest, *Sp1* could regulate miR-365, which is involved in the NF-κB pathway (Xu *et al.*, 2011b), whereas NF-κB has been shown to play a major role in lipopolysaccharide-induced expression of interleukin-6 and other inflammatory cytokines (Luedde and Schwabe, 2011). In our study, knockdown of *Sp1* expression decreased cell proliferation, migration, and invasion, the same as observed with increased levels of the miR-1188. More significantly, the relationship between miR-1188 and Sp1 was identified by Western blot of cells cotransfected with mimics or inhibitor and siRNAs. In the inhibitor groups, even if there was an *Sp1* interference fragment, miR-1188 knockdown still rescued the expression of Sp1. Moreover, we analyzed the negative correlation of the expression levels of miR-1188 and *Sp1* in vivo. Collectively our data suggest that in HCC, miR-1188 mediates invasion by the modulation of Sp1 levels. Thus miR-1188 might be linked with inflammatory pathways by targeting *Sp1* as well as other pathways in liver cells.

Next we found that enhanced miR-1188 could dramatically induce apoptosis of hepatoma cells. Previous studies showed that proteins in the *Bcl-2* family are central regulators of programmed cell death (Lessene *et al.*, 2008), and *p53* acts as a tumor suppressor in many tumor types. First, we detected the expression of Bcl2, Bax, and p53. Of interest, enhanced miR-1188 decreased Bcl-2 protein levels and increased Bax and p53 protein levels. By using a bioinformatic analysis, we confirmed that *Bcl-2* was a target of miR-1188. Furthermore, suppression of *Bcl-2* by siRNA promoted apoptosis, and miR-1188 inhibitor led to reduced apoptosis, whereas miR-1188 inhibitor rescued apoptosis caused by suppression of *Bcl-2* in cells cotransfected with inhibitor and siRNA. Moreover, the relationship between miR-1188 and *Bcl-2* was also identified by Western blot in cells cotransfected with mimics or inhibitor and siRNAs. This confirmed that miR-1188 indirectly targeted *Bcl-2* and was involved in hepatoma cell apoptosis. The mechanism by which miR-1188 regulates *p53* in hepatocellular carcinoma needs to be addressed in further studies. We speculate that *p53* is involved in another apoptosis pathway that causes miR-1188 to induce hepatoma cell apoptosis (Figure 6H).

Although we found that *Bcl-2* and *Sp1* are involved in miR-1188–mediated hepatocellular carcinoma progression, *Bcl-2* or *Sp1* knockdown did not completely abolish the effects of miR-1188 knockdown, suggesting that other genes regulated by miR-1188 may contribute to inhibition of apoptosis and invasion by miR-1188. Therefore we further determined the expression profile of miR-1188–regulated genes. Many tumorigenesis-related genes involved in apoptosis and invasion were induced at enhanced levels in cells with elevated miR-1188, including *Vegfa*, *Fgfr1*, and *Rprd1b*. They are all proto-oncogenes involved in cell proliferation, migration, and apoptosis (Wang *et al.*, 2013; Zhou *et al.*, 2013). *Rprd1b* was shown to enhance the transcription of CCND1 and promote the transcriptional activity of the β-catenin–TCF4 complex in response to *Wnt* signaling (Zhang *et al.*, 2014). In the present study, enhanced miR-1188 decreased the expression of CCND1 (unpublished data), which suggested that *Rprd1b* might be a putative miR-1188 target. Certainly, genes up-regulated by enhanced miR-1188, such as CD44, *Dapk1*, and *Apaf1*, have a tumor suppressor function (Haraguchi *et al.*, 2000; Lee *et al.*, 2005; Williams *et al.*, 2013). In addition, *Bcl-2* suppressed *Apaf1*-independent cell death (Haraguchi *et al.*, 2000). The correlation between miR-1188 and these genes during the course of hepatocellular carcinoma needs to be addressed in further studies.

In summary, this work investigated the potential role of miR-1188 in tumorigenesis and its underlying mechanisms. The data suggest that down-regulation of miR-1188 might play an important role in the development of liver cancer and that miR-1188 might be used as a prognostic marker and therapeutic target for hepatocellular carcinoma.

MATERIALS AND METHODS

Cell line and cell culture

Mouse HCC cell line Hepa1-6 was provided by the Institute of Biochemistry and Cell Biology of the Chinese Academy of Science (Shanghai, China) and originated from the American Type Culture Collection (Manassas, VA). Cells were cultured in DMEM with 10% fetal bovine serum and 2 mM L-glutamine (Corning, Corning, NY). The cell line was incubated at 37°C under a 5% CO_2 atmosphere.

RNA isolation and qRT-PCR

Total RNAs were isolated from mouse liver tissues and Hepa1-6 cell lines using TRIzol reagent (Invitrogen, Carlsbad, CA) and a mirVana miRNA Isolation Kit (Applied Biosystems, Foster City, CA). The expression of miR-1188 was analyzed by TaqMan miRNA assays according to the manufacturer's protocols (Applied Biosystems) using *RNU6B* as an endogenous control. The mRNA expression of *Bcl-2*/*Sp1* was analyzed by SYBR qPCR assays (Applied Biosystems) using β-actin as an endogenous control. The comparative threshold cycle (C_T) method was used to quantify the target genes relative to the endogenous control. Primers used for PCR are listed in Supplemental Table S1.

MiRNA and siRNA transfections

All miRNAs and siRNAs, including negative controls (scrambled RNAs), were chemically synthesized by GenePharma (Shanghai, China) and transfected into Hepa1-6 cells at a final concentration of 25, 50, or 100 nM with Lipofectamine 2000 (Invitrogen). Sequences are listed in Supplemental Table S2.

MTT and colony formation assays

Hepa1-6 cells at 24 h posttransfection were seeded at 2×10^3 cells/well in 96-well plates and the procedure was repeated after 24, 48, 72, and 96 h. Ten microliters of MTT was added to 100 µl of culture medium/well. After 4 h of incubation at 37°C, the medium was removed and 150 µl of dimethyl sulfoxide was added. The absorbance was measured at a wavelength of 490 nm in a plate reader (Bio-Rad, Hercules, CA). Soft agar colony formation was performed as described previously and measured after 10 d (Stephenson *et al.*, 1971). Each assay was performed in triplicate.

Wound-healing, cell migration, and invasion assays

Confluent monolayer cells were scratched with a 200-µl pipette tip and then washed with phosphate-buffered saline (PBS) to clear cell debris. Fresh serum-free medium was added, and the cells were allowed to close the wound for 24 h.

Cells (3×10^4) with the indicated transfections were plated on the top side of Transwell chambers (Corning) coated with or without Matrigel (BD Biosciences, San Diego, CA). After incubation for 48 h, cells were removed from the upper chamber with cotton swabs while the lower surface cells were fixed with 4% paraformaldehyde (PFA) at room temperature for 30 min and stained with 0.1% crystal violet for 20 min. Five independent fields were counted under the microscope (BX51; Olympus, Tokyo, Japan). Each assay was performed in triplicate.

Caspase-3 activity assay

The activity of caspase-3 was determined using a caspase-3 activity kit (Beyotime, Beijing, China) according to the manufacturer's instructions. Cell lysates at 24 or 48 h posttransfection were assessed in 96-well microtiter plates by incubating 10 µl of protein of cell lysate/sample in 80 µl of reaction buffer containing 10 µl of caspase-3 substrate (Ac-DEVD-pNA). Lysates were incubated at 37°C for 4 h, and then the samples were measured at a wavelength of 405 nm in a plate reader (Bio-Rad). Each assay was performed in triplicate.

Flow cytometric assay

Hepa1-6 cells at 20 h posttransfection were washed twice with cold PBS and then resuspended. Cells were suspended in 1× binding buffer (BD Biosciences) at a concentration of 1×10^6 cells/ml. Then 100 µl of the solution (1×10^5 cells) was transferred to a 5-ml culture tube; 5 µl of fluorescein isothiocyanate (FITC)–Annexin V and 5 µl of propidium iodide (PI) were added, and the mixture was incubated for 15 min at room temperature in the dark. Finally, 400 µl of 1× binding buffer was added to the tube, and the samples were analyzed by flow cytometry (FACSCantoII; BD Biosciences). The data were analyzed using FlowJo software. Each assay was performed in triplicate.

Plasmid construction and luciferase reporter assays

Wild-type and mutant 3′-UTRs were amplified from mouse cDNA using the primers listed in Supplemental Table S1. Mutations in miRNA target sites were generated using the KOD-Plus-Mutagenesis Kit (Toyobo, Japan). Target fragments were cloned into the pMIR-REPORT luciferase vector (Ambion, Austin, TX), to produce pMIR-*Bcl-2*/*Sp1*-3′UTR-WT and pMIR-*Bcl-2*/*Sp1*-3′UTR-mut. Hepa1-6 cells were seeded into 24-well plates and cotransfected with 0.5 µg of the appropriate pMIR-REPORT luciferase vector, 0.05 µg of pRL-TK *Renilla* luciferase vector, and 100 nM miR-1188 mimics or stable negative control, using Lipofectamine 2000. After 48 h of transfection, luciferase activity was measured using the dual luciferase reporter assay system (Promega, Madison, WI). Each assay was performed in triplicate.

Western blot analysis

Cells in six-well plates at 48 h posttransfection were lysed with RIPA buffer. A total of 20–40 µg of whole protein was run on 7.5% SDS–PAGE and transferred onto polyvinylidene fluoride membrane. The membrane was blocked and then incubated with primary antibodies overnight at 4°C. In this study, we used antibodies including Bcl-2, Bax, P53, β-actin (Cell Signaling Technology, Beverly, MA), and Sp1 (Abcam, Cambridge, United Kingdom). Quantitative western blot was performed using an Odyssey infrared imaging system (LI-COR, Lincoln, NE).

Immunofluorescence

Hepa1-6 cells were cultured on 24-well chamber slides and fixed with 4% PFA for 30 min. The slides were washed in PBS three times and incubated at 4°C overnight with antibody against Sp1 or F-actin diluted 1:2500 in 3% bovine serum albumin (BSA)/PBS. After washing with PBS and incubation at 37°C for 2 h with anti-FITC antibodies diluted 1:1000 in 1% BSA/PBS, the slides were incubated with 4′,6-diamidino-2-phenylindole (DAPI; Invitrogen) and examined using a fluorescence microscope (Olympus).

Immunohistochemistry and in situ hybridization

Tissues were fixed in 4% PFA and embedded in paraffin blocks. Sections (3 µm) were used for examination. Sp1 expression was detected following the protocol described in *Immunofluorescence*. In situ hybridization was performed using methods described previously (Huang *et al.*, 2013). MiR-1188 LAN probes (Exiqon; http://Exiqon.com) were labeled with a DIG-3′-end labeling kit (Roche, Mannheim, Germany) according to the manufacturer's instructions. An antisense LNA probe for miR-1188, with sequence TGGTGTGAGGTTGGGCCAGGA, was purchased from Exiqon. Sense probes were used as negative controls for all experiments. The signal was detected by incubation with anti-FITC antibodies (1:1000; Invitrogen). Nuclei were stained with DAPI. The images were recorded with a confocal microscope (Zeiss, Jena, Germany).

In vivo assay

Six-week-old female BALB/C athymic mice were used for examining tumorigenicity. Cells (5×10^6) at 48 h posttransfection were resuspended in 100 µl of PBS and implanted into the left and right flanks by subcutaneous injection. The volume of the tumor developed was measured with a caliper every 4 d for 18 d, and the tumor volume was calculated according to volume = (length × width^2)/2. All animal procedures were performed according to protocols approved by the Rules for Animal Experiments published by the Chinese Government (Beijing, China).

Microarray analysis

Total RNA was extracted from Hepa1-6 cells transfected with miR-1188 mimics and stable negative control using TRIzol. Microarray analysis was performed by Genergy Bio (JingNeng, Shanghai, China). The DAVID Bioinformatics Resources database was used to perform gene function enrichment analysis.

Statistical analysis

Data are presented as the mean ± SEM of at least three independent experiments. Two-tailed Student's *t* test and one-way analysis of variance were used to analyze significant differences. We performed Spearman's correlation analysis between miRNAs and their corresponding targets. $p < 0.05$, $p < 0.01$, and $p < 0.001$ were considered statistically significant.

ACKNOWLEDGMENTS

This work was supported by funding from the National Natural Science Foundation of China (Grants 31371478, 31171383, 31100934, and 31100928), the State Key Laboratory of Urban Water Resource and Environment, Harbin Institute of Technology (No. 2013DX07), the Natural Science Foundation of Heilongjiang Province (Grant QC2014C016), and the Innovation and Technology Special Fund for Researchers of Harbin City (Grant 2013RFXXJ010).

REFERENCES

Aravalli RN, Steer CJ, Cressman EN (2008). Molecular mechanisms of hepatocellular carcinoma. Hepatology 48, 2047–2063.

Banerjee N, Talcott S, Safe S, Mertens-Talcott SU (2012). Cytotoxicity of pomegranate polyphenolics in breast cancer cells in vitro and vivo: potential role of miRNA-27a and miRNA-155 in cell survival and inflammation. Breast Cancer Res Treat 136, 21–34.

Benetatos L, Hatzimichael E, Londin E, Vartholomatos G, Loher P, Rigoutsos I, Briasoulis E (2013). The microRNAs within the DLK1-DIO3 genomic region: involvement in disease pathogenesis. Cell Mol Life Sci 70, 795–814.

Cha C, Dematteo RP (2005). Molecular mechanisms in hepatocellular carcinoma development. Best Pract Res Clin Gastroenterol 19, 25–37.

Cimmino A, Calin GA, Fabbri M, Iorio MV, Ferracin M, Shimizu M, Wojcik SE, Aqeilan RI, Zupo S, Dono M, *et al.* (2005). miR-15 and miR-16 induce apoptosis by targeting BCL2. Proc Natl Acad Sci USA 102, 13944–13949.

Denoyelle C, Lambert B, Meryet-Figuiere M, Vigneron N, Brotin E, Lecerf C, Abeilard E, Giffard F, Louis MH, Gauduchon P, *et al.* (2014). miR-491–5p-induced apoptosis in ovarian carcinoma depends on the direct inhibition of both BCL-XL and EGFR leading to BIM activation. Cell Death Dis 5, e1445.

Fang Z, Fu Y, Liang Y, Li Z, Zhang W, Jin J, Yang Y, Zha X (2007). Increased expression of integrin beta1 subunit enhances p21WAF1/Cip1 transcription through the Sp1 sites and p300-mediated histone acetylation in human hepatocellular carcinoma cells. J Cell Biochem 101, 654–664.

Gattolliat CH, Thomas L, Ciafre SA, Meurice G, Le Teuff G, Job B, Richon C, Combaret V, Dessen P, Valteau-Couanet D, *et al.* (2011). Expression of miR-487b and miR-410 encoded by 14q32.31 locus is a prognostic marker in neuroblastoma. Br J Cancer 105, 1352–1361.

Glazov EA, McWilliam S, Barris WC, Dalrymple BP (2008). Origin, evolution, and biological role of miRNA cluster in DLK-DIO3 genomic region in placental mammals. Mol Biol Evol 25, 939–948.

Guo LH, Li H, Wang F, Yu J, He JS (2013). The tumor suppressor roles of miR-433 and miR-127 in gastric cancer. Int J Mol Sci 14, 14171–14184.

Haraguchi M, Torii S, Matsuzawa S, Xie Z, Kitada S, Krajewski S, Yoshida H, Mak TW, Reed JC (2000). Apoptotic protease activating factor 1 (Apaf-1)-independent cell death suppression by Bcl-2. J Exp Med 191, 1709–1720.

Huang Z, Han Z, Cui W, Zhang F, He H, Zeng T, Sugimoto K, Wu Q (2013). Dynamic expression pattern of Pde4d and its relationship with CpG methylation in the promoter during mouse embryo development. Biochem Biophys Res Commun 441, 982–987.

Iliopoulos D, Bimpaki EI, Nesterova M, Stratakis CA (2009). MicroRNA signature of primary pigmented nodular adrenocortical disease: clinical correlations and regulation of Wnt signaling. Cancer Res 69, 3278–3282.

Janumyan YM, Sansam CG, Chattopadhyay A, Cheng N, Soucie EL, Penn LZ, Andrews D, Knudson CM, Yang E (2003). Bcl-xL/Bcl-2 coordinately regulates apoptosis, cell cycle arrest and cell cycle entry. EMBO J 22, 5459–5470.

Jewer M, Findlay SD, Postovit LM (2012). Post-transcriptional regulation in cancer progression: microenvironmental control of alternative splicing and translation. J Cell Commun Signal 6, 233–248.

Kelly PN, Strasser A (2011). The role of Bcl-2 and its pro-survival relatives in tumourigenesis and cancer therapy. Cell Death Differ 18, 1414–1424.

Lee JH, Rho SB, Chun T (2005). Programmed cell death 6. (PDCD6) protein interacts with death-associated protein kinase 1 (DAPk1): additive effect on apoptosis via caspase-3 dependent pathway. Biotechnol Lett 27, 1011–1015.

Lessene G, Czabotar PE, Colman PM (2008). BCL-2 family antagonists for cancer therapy. Nat Rev Drug Discov 7, 989–1000.

Lietard J, Musso O, Theret N, L'Helgoualc'h A, Campion JP, Yamada Y, Clement B (1997). Sp1-mediated transactivation of LamC1 promoter and coordinated expression of laminin-gamma1 and Sp1 in human hepatocellular carcinomas. Am J Pathol 151, 1663–1672.

Liu JJ, Lin XJ, Yang XJ, Zhou L, He S, Zhuang SM, Yang J (2014). A novel AP-1/miR-101 regulatory feedback loop and its implication in the migration and invasion of hepatoma cells. Nucleic Acids Res 42, 12041–12051.

Lou Z, O'Reilly S, Liang H, Maher VM, Sleight SD, McCormick JJ (2005). Down-regulation of overexpressed sp1 protein in human fibrosarcoma cell lines inhibits tumor formation. Cancer Res 65, 1007–1017.

Lu C, Huang X, Zhang X, Roensch K, Cao Q, Nakayama KI, Blazar BR, Zeng Y, Zhou X (2011). miR-221 and miR-155 regulate human dendritic cell development, apoptosis, and IL-12 production through targeting of p27kip1, KPC1, and SOCS-1. Blood 117, 4293–4303.

Luedde T, Schwabe RF (2011). NF-kappaB in the liver—linking injury, fibrosis and hepatocellular carcinoma. Nat Rev Gastroenterol Hepatol 8, 108–118.

Luk JM, Burchard J, Zhang C, Liu AM, Wong KF, Shek FH, Lee NP, Fan ST, Poon RT, Ivanovska I, *et al.* (2011). DLK1-DIO3 genomic imprinted microRNA cluster at 14q32.2 defines a stemlike subtype of hepatocellular carcinoma associated with poor survival. J Biol Chem 286, 30706–30713.

Ren LH, Chen WX, Li S, He XY, Zhang ZM, Li M, Cao RS, Hao B, Zhang HJ, Qiu HQ, Shi RH (2014). MicroRNA-183 promotes proliferation and invasion in oesophageal squamous cell carcinoma by targeting programmed cell death 4. Br J Cancer 111, 2003–2013.

Roderburg C, Luedde T (2014). Circulating microRNAs as markers of liver inflammation, fibrosis and cancer. J Hepatol 61, 1434–1437.

Shen G, Rong X, Zhao J, Yang X, Li H, Jiang H, Zhou Q, Ji T, Huang S, Zhang J, Jia H (2014). MicroRNA-105 suppresses cell proliferation and inhibits PI3K/AKT signaling in human hepatocellular carcinoma. Carcinogenesis 35, 2748–2755.

Stephenson JR, Axelrad AA, McLeod DL, Shreeve MM (1971). Induction of colonies of hemoglobin-synthesizing cells by erythropoietin in vitro. Proc Natl Acad Sci USA 68, 1542–1546.

Su R, Lin HS, Zhang XH, Yin XL, Ning HM, Liu B, Zhai PF, Gong JN, Shen C, Song L, *et al.* (2014). MiR-181 family: regulators of myeloid differentiation and acute myeloid leukemia as well as potential therapeutic targets. Oncogene, doi: 10.1038/onc.2014.274.

Swarbrick A, Woods SL, Shaw A, Balakrishnan A, Phua Y, Nguyen A, Chanthery Y, Lim L, Ashton LJ, Judson RL, *et al.* (2010). miR-380-5p represses p53 to control cellular survival and is associated with poor outcome in MYCN-amplified neuroblastoma. Nat Med 16, 1134–1140.

Tryndyak VP, Ross SA, Beland FA, Pogribny IP (2009). Down-regulation of the microRNAs miR-34a, miR-127, and miR-200b in rat liver during hepatocarcinogenesis induced by a methyl-deficient diet. Mol Carcinog 48, 479–487.

Wang J, Li J, Wang X, Zheng C, Ma W (2013). Downregulation of microRNA-214 and overexpression of FGFR-1 contribute to hepatocellular carcinoma metastasis. Biochem Biophys Res Commun 439, 47–53.

Wang SC, Lin XL, Li J, Zhang TT, Wang HY, Shi JW, Yang S, Zhao WT, Xie RY, Wei F, *et al.* (2014). MicroRNA-122 triggers mesenchymal-epithelial transition and suppresses hepatocellular carcinoma cell motility and invasion by targeting RhoA. PLoS One 9, e101330.

Williams K, Motiani K, Giridhar PV, Kasper S (2013). CD44 integrates signaling in normal stem cell, cancer stem cell and (pre)metastatic niches. Exp Biol Med (Maywood) 238, 324–338.

Xia L, Zhang D, Du R, Pan Y, Zhao L, Sun S, Hong L, Liu J, Fan D (2008). miR-15b and miR-16 modulate multidrug resistance by targeting BCL2 in human gastric cancer cells. Int J Cancer 123, 372–379.

Xie C, Jiang XH, Zhang JT, Sun TT, Dong JD, Sanders AJ, Diao RY, Wang Y, Fok KL, Tsang LL, *et al.* (2013). CFTR suppresses tumor progression through miR-193b targeting urokinase plasminogen activator (uPA) in prostate cancer. Oncogene 32, 2282–22912291.e1–7.

Xiong Y, Fang JH, Yun JP, Yang J, Zhang Y, Jia WH, Zhuang SM (2010). Effects of microRNA-29 on apoptosis, tumorigenicity, and prognosis of hepatocellular carcinoma. Hepatology 51, 836–845.

Xu D, Takeshita F, Hino Y, Fukunaga S, Kudo Y, Tamaki A, Matsunaga J, Takahashi RU, Takata T, Shimamoto A, *et al.* (2011a). miR-22 represses cancer progression by inducing cellular senescence. J Cell Biol 193, 409–424.

Xu WP, Yi M, Li QQ, Zhou WP, Cong WM, Yang Y, Ning BF, Yin C, Huang ZW, Wang J, *et al.* (2013). Perturbation of MicroRNA-370/Lin-28 homolog A/nuclear factor kappa B regulatory circuit contributes to the development of hepatocellular carcinoma. Hepatology 58, 1977–1991.

Xu Y, Zhao F, Wang Z, Song Y, Luo Y, Zhang X, Jiang L, Sun Z, Miao Z, Xu H (2012). MicroRNA-335 acts as a metastasis suppressor in gastric cancer by targeting Bcl-w and specificity protein 1. Oncogene 31, 1398–1407.

Xu Z, Xiao SB, Xu P, Xie Q, Cao L, Wang D, Luo R, Zhong Y, Chen HC, Fang LR (2011b). miR-365, a novel negative regulator of interleukin-6 gene expression, is cooperatively regulated by Sp1 and NF-kappaB. J Biol Chem 286, 21401–21412.

Yang H, Huang ZZ, Wang J, Lu SC (2001). The role of c-Myb and Sp1 in the up-regulation of methionine adenosyltransferase 2A gene expression in human hepatocellular carcinoma. FASEB J 15, 1507–1516.

Yang Z, Tsuchiya H, Zhang Y, Hartnett ME, Wang L (2013a). MicroRNA-433 inhibits liver cancer cell migration by repressing the protein expression and function of cAMP response element-binding protein. J Biol Chem 288, 28893–28899.

Yang Z, Zhang Y, Wang L (2013b). A feedback inhibition between miRNA-127 and TGFbeta/c-Jun cascade in HCC cell migration via MMP13. PLoS One 8, e65256.
Yang Y, Wu J, Guan H, Cai J, Fang L, Li J, Li M (2012). MiR-136 promotes apoptosis of glioma cells by targeting AEG-1 and Bcl-2. FEBS Lett 586, 3608–3612.
Yasuda K, Hirayoshi K, Hirata H, Kubota H, Hosokawa N, Nagata K (2002). The Kruppel-like factor Zf9 and proteins in the Sp1 family regulate the expression of HSP47, a collagen-specific molecular chaperone. J Biol Chem 277, 44613–44622.
Zhang Y, Liu C, Duan X, Ren F, Li S, Jin Z, Wang Y, Feng Y, Liu Z, Chang Z (2014). CREPT/RPRD1B, a recently identified novel protein highly expressed in tumors, enhances the beta-catenin.TCF4 transcriptional activity in response to Wnt signaling. J Biol Chem 289, 22589–22599.
Zhang Y, Wu L, Wang Y, Zhang M, Li L, Zhu D, Li X, Gu H, Zhang CY, Zen K (2012). Protective role of estrogen-induced miRNA-29 expression in carbon tetrachloride-induced mouse liver injury. J Biol Chem 287, 14851–14862.
Zhou B, Ma R, Si W, Li S, Xu Y, Tu X, Wang Q (2013). MicroRNA-503 targets FGF2 and VEGFA and inhibits tumor angiogenesis and growth. Cancer Lett 333, 159–169.